

Quasi-universal relations in the context of future neutron star detections

Lami Suleiman* and Jocelyn Read

*Nicholas and Lee Begovich Center for Gravitational Wave Physics and Astronomy,
California State University Fullerton, Fullerton, California 92831, USA.*

(Dated: February 7, 2024)

The equation of state dependence of neutron star's astrophysical features modeling is key to our understanding of isospin asymmetric and dense matter. However, there exists a series of almost equation-of-state independent relations reported in the literature, called quasi-universal relations, that are used to determine neutron star radii and moments of inertia from X-ray and gravitational wave signals. Using sets of equations of state constrained by multi-messenger astronomy measurements and nuclear-physics theory, we discuss quasi-universal relations in the context of future gravitational-wave detectors Cosmic Explorer and Einstein Telescope, and X-ray detector STROBE-X. We focus on relations that involve the moment of inertia I , the tidal deformability Λ and the compactness C : $C(\Lambda)$, $I(\Lambda)$ and $I(C)$. The quasi-universal fits and their associated errors are constructed with three different microphysics approaches which include state of the art nuclear physics theory and astrophysical constraints. Gravitational-wave and X-ray signals are simulated with the sensitivity of the next generation of detectors. Equation of state inference on those simulated signals is performed to assess if quasi-universal relations will offer a better precision on the extraction of neutron star's macroscopic parameters than equation of state dependent relations. We confirm that the relation $I(\Lambda)$ offers a more pronounced universality than relations involving the compactness regardless of the equation of state set. We show that detections with the 3rd generation of gravitational wave detectors and the X-ray detector STROBE-X will be sensitive to the fit error marginalization technique. We also find that the sensitivity of those detectors will be sufficient that using full equation of state distributions will offer better precision on extracted parameters than quasi-universal relations. We also note that nuclear physics theory offers a more pronounced equation of state invariance of quasi-universal relations than current astrophysical constraints.

I. INTRODUCTION

As the densest stars in the Universe, neutron stars are particularly well suited to investigate ultra-dense matter. Our understanding of the innermost layers of neutron stars remains uncertain due to limitations of nuclear physics laboratories to reach equivalent regimes of temperature and density. Neutron star astrophysical features strongly depend on the equation of state of ultra-dense matter, thus offering the opportunity to probe the neutron star interior with multi-messenger astronomy. On the other hand, a series of relations between various neutron star observables, referred to as quasi (or almost) universal relations, were empirically found to depend weakly on the exact equation of state [1].

While the perfectly holding universality (as per the no-hair theorem) of isolated and stationary black holes in the gravitational theory of General Relativity is in principle not applicable to compact stars, their external gravitational field presents features that are almost independent of the neutron star's interior. This (almost) universality applies to non-magnetized neutron stars on a static metric in General Relativity and holds for magnetized [2] and spinning neutron stars [3], as well as in modified gravity theories [4]. The underlying physics of this universality has been connected to approximate

no-hair relations, where high order multiple moments of compact stars are approximately determined by low order multipole moments, and to the self-similarity of isodensities in compact star. For a detailed introduction and history of universality in compact stars, as well as the derivation of the approximate no-hair relations, details on the I-Love-Q relations and also on the black-hole limit of this almost universality, we refer to the extensive review and work of Ref. [5] and references therein.

The era of multi-messenger astronomy has allowed for the detection of various neutron star's astrophysical features and is expected to provide increasingly more precise observational data in the future. Almost equation of state independent relations between macroscopic parameters of neutron stars are well suited to extract the astrophysical detection of one parameter from the measure of another (or others). The measurement of post-Keplerian parameters in binary systems via pulsar timing has provided the most precise measurements of neutron star's gravitational mass M . Various wavelength of the electromagnetic spectrum (radio, X-ray and optics) as well as gravitational wave signals from binary neutron star mergers have provided a large number of mass measurements¹. The Neutron star Interior Composition

* lsuleiman@fullerton.edu

¹ For a list of neutron star masses measurements with reported precision, see <https://compose.obspm.fr/resources>.

Explorer (NICER) telescope, which relies on the effects of General Relativity on the detection of hot spots on the surface of a rotating neutron star, has provided the simultaneous measurement of both the gravitational mass and the radius R for two sources (J0030+0451 and J0740+6620) [6–9]. Although the precision of the NICER telescope has made some constraint on the equation of state of dense matter, the future Spectroscopic Time-Resolving Observatory for Broadband Energy X-rays (STROBE-X) [10] is expected to offer measurements of mass-radius contours two to three times tighter. The tidal deformability Λ of a neutron star was for the first time from the gravitational wave measurement of the double neutron star binary merger source GW170817 [11]. The significant increase in sensitivity brought forth by the next generation of gravitational wave detectors, such as the Cosmic Explorer [12] and the Einstein Telescope [13, 14], is expected to increase the number and precision of detections by several orders of magnitude. Double pulsar binaries are the most promising systems to detect the star’s moment of inertia I ; the famous double pulsar PSR J0737-3039 for which more than 15 years of data was gathered [15] has not permitted the direct measurement of the moment of inertia yet. However, Ref. [16] have been able to use a quasi-universal relation that involves I , M and Λ to extract constraints on the moment of inertia of J0737–3039A.

In this paper, we assess the quasi-universality of three relations and discuss their use in the context of next generation of detectors. In Section II, the quasi-universal relations used in this paper and the equation of state sets on which they are based are discussed. We then give details on quasi-universal relations fits and how to introduce the equation of state variability as the fit’s error. We show how next-generation detections are simulated. In Section III, we compare the quasi-universal relations designed with different equation of state sets. We then discuss the impact of different marginalizations of the fit error on the extraction of neutron star’s macroscopic parameters. We contrast the detector sensitivity with the equation of state variability of quasi-universal relations. Finally, we use equation of state inference to compare the accuracy of parameter extraction with quasi-universal relations and equation of state dependent relations. In the Appendix, we present the mass, radius, tidal deformability and moment of inertia modeling, as well as parameters for the quasi-universal relation fits.

II. METHODS

In this paper, we explore astrophysical features of a neutron star within the theory of General Relativity, assuming the line element of a spherically symmetric, static and isotropic space-time. The mass M and radius R are solved using the Tolman-Oppenheimer-Volkov

[17, 18] differential equations. The moment of inertia I is determined in the slow-rotation approximation of Ref. [19] and the tidal deformability follows the Ref. [20] derivation. For details on the modeling of macroscopic parameters, see Appendix A.

A. Quasi-universal relations

1. $C(\Lambda)$, $I(\Lambda)$ and $I(C)$

In this paper, we study the following relations:

1. The relation between the compactness and the dimensionless tidal deformability $C(\Lambda)$, with $C = GM/(Rc^2)$. In the assumption that this relation is equation of state independent, it can be used to extract the radius of the neutron star from the gravitational wave measurement of its mass and tidal deformability, see e.g., Ref. [21].
2. The relation between the dimensionless moment of inertia $\bar{I} = Ic^4/(G^2M^3)$ and the dimensionless tidal deformability $\bar{I}(\Lambda)$. In the assumption that this relation is equation of state independent, it can be used to extract the moment of inertia from the gravitational wave measurement of the mass and tidal deformability, see e.g., Ref. [16].
3. The relation between the dimensionless moment of inertia and the compactness $\bar{I}(C)$. In the assumption that this relation is equation of state independent, it can be used to extract the moment of inertia from the simultaneous measurement of the mass and radius by telescope such as NICER or Strobe-X, see e.g., Ref. [22].

Not all of the above mentioned relations are equal in the face of equation of state independence (see Ref. [5, 23]), but they are all considered in the literature to be quasi-universal. If the relations hold through equation of state variation, it is also possible to parameterize them with what is referred to as fits, see, e.g., Refs. [1, 5, 24–27] or Section II C 2 of the present paper.

2. Quasi-universal or data driven relations

The universality qualifier attributed to the relations studied in this paper should relate astrophysical features of neutron star’s in spite of the description of the neutron star interior, or in other words the Equation of State (EoS). It should be possible to use minimally constrained EoSs (only causal and thermodynamically consistent) and still retain the quasi-universality in the relations. Such relations would reflect the EoS independence driven by General Relativity, not a decreased EoS variability related to our increasing knowledge on the behavior of ultra-dense matter, or

our bias in choosing certain EoSs. The introduction of astrophysical and nuclear constraints on the EoS can appear as stronger universality but would be better described as a data driven narrowing of the EoS dependence.

In this paper, we do not use quasi-universal relations established from minimally constrained EoS sets, but data-driven relations from informed sets. We consider both up to date astrophysical data and nuclear physics data.

B. Equations of state sets

1. Nuclear physics based set

The first set comprises sixty one EoSs established from full nuclear physics calculations. The EoSs are gathered from Ref. [28] to which we add seven EoSs presented in Ref. [29]. They describe cold and catalyzed β -equilibrated matter as such thermodynamic conditions are relevant for isolated “adult” (not proto) neutron stars and for the inspiral phase of a neutron star merger².

The EoSs of this set were computed with two different nuclear physics approaches: relativistic mean field theory (x39), Skyrme force energy density functionals (x22). Among the relativistic mean field models are included ten EoSs with a hyperonic core (for a recent review on hyperonic compact stars, see Ref. [30]) and fourteen hybrid models with a core quark phase transition (see, e.g., Refs. [31, 32]); the rest have nucleonic cores.

All EoSs of this set follow thermodynamic consistency; note that the Skyrme density functional are based on a non-relativistic approach that does not guarantee sound speed causality. They are unified, meaning that the crust (low density) and the core (high density) have been calculated with the same nuclear physics model; we refer to Ref. [33] for a discussion on the role of non-unified EoSs in neutron star modeling. A large majority of them also permit the Direct Urca process, a neutrino emission reaction which X-ray observations indicate exists in neutron stars [34]. They all meet at least the mass constraint imposed by the 1σ pulsar timing measurement of the millisecond pulsar J0740+6620 with a mass of $2.08 \pm 0.07 M_{\odot}$ [35]³. In overall, this set comprises

various core compositions and nuclear approaches, with reasonable microphysics parameters when compared to modern nuclear physics laboratory (see Ref. [33]) and astrophysics measurements while keeping a certain variability in their nuclear physics features.

2. Agnostic sets

The two other sets are based on an agnostic approach, that is to say that the EoSs are not constructed with specific nuclear physics calculations. The point of such sets is to explore the parameter space of pressure and density and to go beyond our usual EoS constructions. In the following, we discuss two agnostic sets: one parametric which we will refer to as the “meta-model” set, and one non parametric, later on referred to as the “Gaussian process” set.

The first of the agnostic sets is based on Ref. [37]. To construct one EoS, the nuclear empirical parameters that are the saturation density, the energy of symmetric matter at saturation density, the symmetry energy, the isoscalar and isovector incompressibility, skewness and kurtosis, the nucleon effective mass and the effective mass isospin are randomly thrown in intervals determined by nuclear physics laboratory experiments. Taking advantage of chiral-effective-field theory calculations presented in Ref. [38] for pure neutron matter, the β -equilibrated EoSs can be constrained. For a given collection of nuclear empirical parameters, the low density part of the EoS is reconstructed according to the meta-modeling approach discussed in Ref. [39], with a compressible liquid drop model for the inhomogeneous crust. The high density part is constructed with five polytropes for which the adiabatic index and the polytropic constant are randomly thrown. The meta-model set, respects thermodynamic consistency, sound speed causality and provides EoSs in accordance with nuclear physics laboratory experiments while keeping the freedom permitted by the unknown core behavior and the error bars of nuclear experiments at low density. It is a parametric approach, that is to say it follows a specific functional, which implements bias. This set is constrained by the pulsar timing mass measurement of the millisecond pulsar J0740+6620, it is composed of 5×10^4 EoSs, and is denoted MM+ χ +PSR.

The second agnostic set is publicly available and constructed with the Gaussian process approach discussed in Ref. [40]. Contrary to a parametric approach, the Gaussian process EoSs are not bound by the functional chosen to parameterize, and therefore avoid the sort of bias inherent to parametrized constructions, e.g., the discontinuous sound speed of piecewise polytropes in the meta-model set. The Gaussian process set is trained on fifty nuclear physics based EoSs; the selection of EoSs constitutes a bias, but the training is believed to be sufficiently loose

² We acknowledge that a global thermodynamic equilibrium (catalyzed) neutron star crust may not be appropriate to describe some of the potential STROBE-X sources located in accreting binaries, but nevertheless we reasonably neglect the impact of an accreted crust on the modeling of macroscopic parameters.

³ In Ref. [28], the mass constraint follows J1614–2230 measured at $1.908 \pm 0.016 M_{\odot}$ [36], which is why in our set we did not include H3, hyperonic DD2 and FSU2H, BSk19, KDE0v1, SKOp and BCPM

that this bias is tamed. The low density part of the EoS is conditioned on the DH crust [41]. This set does not offer a well constrained and well constructed crust and core-crust transition, contrary to the meta-model set and the nuclear physics based set. It follows thermodynamic consistency and sound speed causality. This set of EoSs is constrained by the mass of J0740+6620, NICER measurements and by the tidal deformability measurement of GW170817, we refer to it as GP+astro.

C. Parameter extraction

1. Parameter extraction from future astrophysical detections

We refer to parameter extraction as the technique that consists in determining the value of an astrophysical parameter from the measurement of one or several others. To do so, one can either use EoS dependent relations, or quasi EoS independent relations: for example, using a mass measurement we can estimate the radius from the EoS dependent relation $M(R)$, or using a mass and tidal deformability measurement we can estimate the radius from the almost EoS independent relation $C(\Lambda)$.

The reason why the relations presented in Section II A 1 are preferred in parameter extraction is related to the idea that we can count on the universality to retain a tight error bar on the extracted parameter. But in the context of increasing detector precision, we have to assess whether the EoS variability of the relations discussed in this paper overcomes the detector precision. In other words, we shall assess if the quasi-universality or our current state of the art of astrophysics and nuclear physics constrained relations are sufficient for a precise parameter extraction, or if we will have to keep the relations up to date with upcoming EoS constraints.

If the detector precision imposes the use of increasingly data driven relations in parameter extraction, it is also reasonable to question if Section II A 1 relations are still more relevant for parameter extraction than EoS dependent relations. It is important to note that Section II A 1 relations require the detection of at least two parameters to estimate a third, which implies at least two detection errors. EoS dependent relations may involve the detection of only one parameter. Therefore, in the context of increasing detection precision, we have to assess if EoS dependent relations that are sufficiently informed by astrophysical measurements might provide tighter error bars on the extracted parameter than source or data driven relations.

To assess those two points, we simulate neutron-star gravitational and X-ray detections and estimate their associated detection errors:

- A double neutron star binary merger emitting gravitational waves, for which individual masses and tidal deformabilities are recovered with the public parameter estimation software BILBY [42] with ROQ likelihoods [43] suited for third generation telescope analysis [44]. Sky localization parameters of the binary (right ascension and declination) are fixed, or in other words we assume that an electromagnetic counterpart has been found. The spins are aligned, equal and low ($\chi \leq 0.015$) and we consider a binary with a neutron star of mass $M_1 = 1.5 M_\odot$ and a neutron star of mass $M_2 = 1.3 M_\odot$. Tidal deformabilities are calculated from the relation $\Lambda(M)$ determined by the unified equation of state model DD2 [45] as presented in Ref. [33]: $\Lambda_1 \simeq 470$ and $\Lambda \simeq 1055$. Simulations are performed with different detector sensitivities: projected O4 sensitivity of LIGO and Virgo facilities (denoted GW-O4), and third generation telescopes Cosmic Explorer and Einstein Telescope sensitivity (denoted GW-3G)⁴. The signal to noise ratio of this event is quite high ($\simeq 1800$) although not as high as the source presented in Ref. [44].
- An X-ray source with a neutron star mass $M_{\text{xray}} = 1.4 M_\odot$ and a radius established from the equation of state model DD2 $R_{\text{xray}} \simeq 13.16$ km. We use the precision reported in Ref. [7] for the detector sensitivity denoted NICER and the projected sensitivity reported in Ref. [10] denoted STROBE-X, to simulate a distribution of masses and radii using a bi-variate normal distribution peaked on M_{xray} and R_{xray} .

2. Performing fits on agnostic equation of state sets

The usual approach for parameter extraction is to use fits. They correspond to a parametrized function (usually a polynomial) fitted to macroscopic parameters computed with a certain EoS set, and reported with a precision that attests to the largest difference between the fit and the set's macroscopic parameters.

The pertinence of fits based on nuclear physics EoSs to represent the EoS variability in neutron stars must be questioned. First, the different core compositions have an impact on the modeling of macroscopic parameters. The first fits available were based on a limited number of EoS models. For example, the fits presented in Ref. [24] used three EoSs with purely nucleonic cores;

⁴ The sensitivity curves for CE and ET (ET-D design [46]) used to simulate the signal in this paper can be found at <https://dcc.ligo.org/LIGO-T1500293/public>. Updated sensitivity ET-D curves were provided in Ref. [14] recently, but conclusions of our paper remain robust.

the reported precision of 2% for the relation $C(\Lambda)$ was shown in Ref. [33] to be too small when compared to several EoSs of various stiffness. Recognizing that the so called “universal” relations were only quasi-independent of the description of neutron star’s interior, efforts were made to fit to larger sets of nuclear physics based EoSs, including various core compositions thus increasing the reported error of the fits; for example, in Ref. [5], the fits were performed using twenty EoSs with nucleonic cores, seven EoSs with hyperonic or kaon cores and three quark stars; a reported precision of 6.5% is given for neutron stars and 15% for quark stars. Neutron star’s core composition remains unknown, there is therefore no reason to perform the fit on sets containing more nucleonic models than hybrid or hyperonic ones. This is however what is done in practice, systematically with fits based on nuclear physics EoS, likely because nucleonic cores are easily accessible in the literature. A similar reasoning applies to the nuclear physics approach used to establish the set of EoSs on which the fits are based on: relativistic mean field based models tend to be stiffer than e.g., Skyrme energy density functional models. Secondly, there is no reason to reduce the set of EoSs to known hypothesis of the core composition nor our approaches of nuclear physics. To that end, the more relevant set of EoSs to perform the fits should be agnostic, as presented e.g. in Ref. [23, 25].

In this paper, we perform fits of the three relations presented in Section II A 1 with the different EoS sets presented in this paper. For each relation and each set, a non-linear least square method is used to determine the parameter a_k with $k \in [0, 5]$ in

$$C_{\text{fit}} = \sum_{k=0}^5 a_k (\ln \Lambda)^k, \quad (1)$$

$$\ln \bar{I}_{\text{fit}} = \sum_{k=0}^5 a_k \ln(\Lambda)^k, \quad (2)$$

$$\bar{I}_{\text{fit}} = \sum_{k=0}^5 a_k C^{-k}. \quad (3)$$

An error is associated to each fit and denoted $(\Delta X_{\text{fit}})^S$ with X the fitted quantity and S the set of EoSs. The fits are performed using macroscopic parameters of neutron star with at least a mass of $1.0 M_\odot$ up to the last stable mass configuration. The error is assessed from the full range of the (finite) nuclear set, and the 99% percentiles of the GP+astro set and MM+ χ +PSR set. The fit parametrizations for $C(\Lambda)$, $I(\Lambda)$ and $\bar{I}(C)$ presented in Ref. [5] (later denoted Yagi & Yunes) are also used as a comparison.

3. Marginalization of the error

To include the fit error $(\Delta X_{\text{fit}})^S$ in the extraction of a parameter, we must specify a marginalization

technique. This can be done by defining an extra variable δX with a random distribution reflecting the fit uncertainty, such that each sample fitted parameter is multiplied by a factor $(1 + \delta X_{\text{fit}}^S)$. In this paper, we describe this distribution in relation to the error on the fit for a given relation $(\Delta X_{\text{fit}})^S$. For example, in Refs. [11, 47], the marginalization consisted of drawing the fit error parameter δX from a Gaussian function peaked on the fitted relation with a $(\Delta C_{\text{fit}})^{yy}$ variance; with the fit’s error assigned to a $3\text{-}\sigma$ precision, the standard deviation for the Gaussian distribution is $(\Delta X_{\text{fit}})^S/3$. We refer to this technique as the Gaussian marginalization.

In the absence of information on the distribution of macroscopic parameters computed from the EoS set used to perform the fit, we propose that users choose a uniform distribution instead of a Gaussian one: $\delta X_{\text{fit}}^S \in [-(\Delta X_{\text{fit}})^S; (\Delta X_{\text{fit}})^S]$ is randomly drawn from a uniform distribution; this approach is referred to later on as the uniform marginalization. It leads to a larger systematic error on the extraction of the macroscopic parameter but avoids the fit line bias. To illustrate that the distribution of points is not necessarily a Gaussian for a given set of EoS, we present the distribution of compactness and dimensionless moment of inertia around the fit for equation of state sets in Appendix B.

One can also assess the full extent of the fit error. We take the two extremes of the relation $X_{\text{fit}\pm}^S(Z) = X_{\text{fit}}^S(Z) \pm (\Delta X_{\text{fit}})^S$. We then perform the parameter extraction and obtain two distributions which represent the two extremes of the fit error; we refer to this approach as the fit limits.

D. Equation of state inference

Astrophysical sources inform the EoS: sources such as the simulated ones presented Section II C 1 therefore have the potential to constrain the sets of EoSs presented in Section II B. We use the following EoS inference approaches.

For the X-ray simulation, we use a simple likelihood estimation on the $1\text{-}\sigma$ STROBE-X sensitivity data and the MM+ χ +PSR and GP+astro sets. For the gravitational wave simulated data, we use the EoS inference technique discussed in Refs. [40, 48–50] with the software Likelihood Weighting Protocol (LWP⁵) to infer on the MM+ χ +PSR and GP+astro set with the two neutron stars of the binary coalescence in Cosmic Explorer and Einstein Telescope sensitivity.

With this newly informed sets of EoSs, we can extract parameters from the EoS $M(R)$ and $M(I)$ and compare the EoS dependent parameter extraction to data-driven relation technique.

⁵ <https://git.ligo.org/reed.essick/lwp>

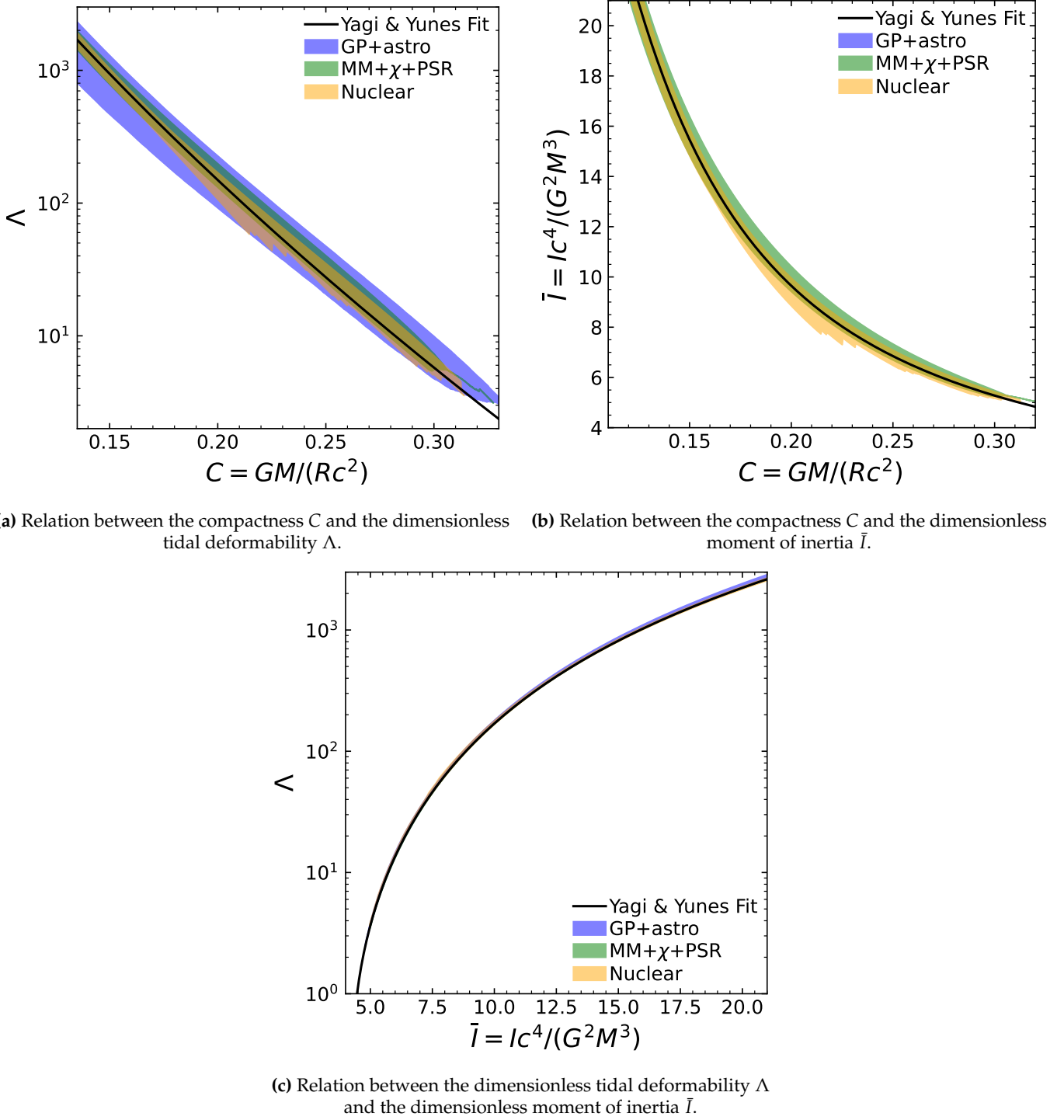


FIG. 1: Contours (99 percentile) presented for the nuclear set, MM+ χ +PSR set and the GP+astro set. In black we present the Yagi & Yunes fit [5].

III. RESULTS

A. Comparison of the different equation of state sets

In Fig. 1 we present the relations of Section II A 1 established from different sets of EoS: the nuclear set,

the GP+astro and the MM+ χ +PSR set. In black is also presented the fits of Yagi & Yunes.

The agnostic GP+astro set presents the largest EoS variability. It explores a larger astrophysics parameter space than the nuclear set and the agnostic MM+ χ +PSR set, and overlaps them both, thus showing that the

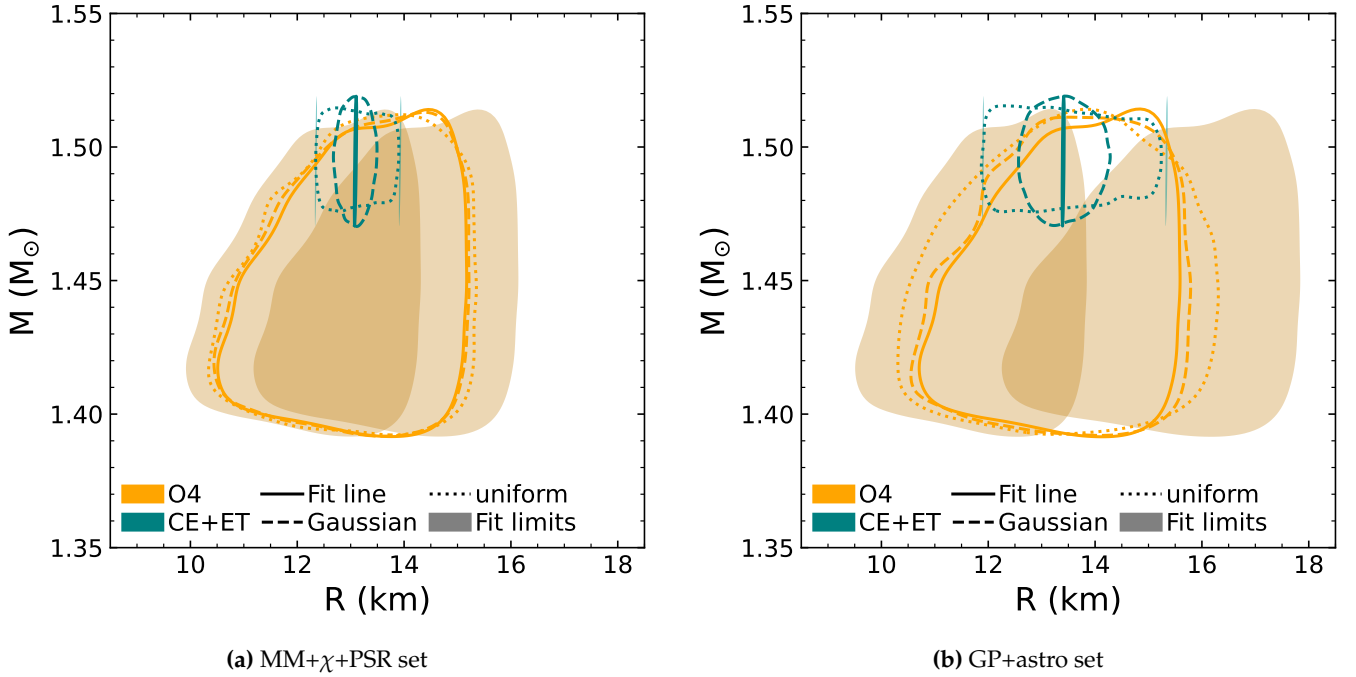


FIG. 2: $M(R)$ extracted from the $C(\Lambda)$ relation and a simulated GW signal in the sensitivity of O4 (orange) and Cosmic Explorer and Einstein telescope (green); contours are shown at $1-\sigma$. Results are presented for the fit line (plain lines), with the Gaussian marginalization of the error (dashed line), and with the uniform marginalization of the error (dotted line); the limits of the error are presented in shades of colors.

chiral effective field theory constraints used for the meta-modeling approach offer stronger constraints than current astrophysical measurements from NICER and GW170817. We note also that the GP+astro set does not encompass the meta-model (nor the nuclear) set in a symmetric way, particularly at low compactness: the meta model set favors higher tidal deformabilities and moment of inertia, in other words, stiffer EoSs.

The nuclear set and the meta model do not perfectly overlap, as some of the EoSs used in the nuclear set are not in accordance with chiral effective field theory constraints. The nuclear set is in good accordance with the fit of Yagi & Yunes, which was also based on complete nuclear physics calculation EoSs. The nuclear set was established using 61 EoSs with various core compositions (including deconfined quarks), however it presents a stronger EoS invariance than the Yagi & Yunes fit based on ~ 30 EoSs. For example, the error associated to the Yagi & Yunes fit of $C(\Lambda)$ is of 6.5% and 15% excluding and including quark stars respectively. Our fit for this relation (see Appendix for parameters) gives a 6% maximum error (see Table I in the Appendix) even though it includes a significant portion of hybrid models. The selection of modern EoS which are calibrated to astrophysical and nuclear physics data plays a role in the smaller error (although not significant) of our fit: for example, the set used to establish the Yagi & Yunes fit includes models presenting low radii at fixed mass

(i.e. high tidal deformability and moment of inertia), which microphysics parameters have been reproved by nuclear physics laboratory experiments e.g. WFF1 and WFF2 [51].

The relation $C(\Lambda)$ in Fig. 1a and $\bar{I}(C)$ in Fig. 1b present a clear EoS variability. The relation $\bar{I}(\Lambda)$ in Fig. 1c is EoS invariant to the point that we cannot distinguish differences between the sets of EoSs: this relation is sufficiently strongly universal to overcome the EoS variability emerging from the use of different EoS sets. This result is in accordance with Ref. [23] which quantifies the degree of universality of various relations: we also find sub-percent errors on the fits (see Table I in the Appendix). Contrary to the compactness involved relations in which the different sets and their various EoS constraints can be distinguished, the $\bar{I}(\Lambda)$ universality cannot be attributed to our use of data driven EoS sets.

The particular EoS invariance of the relation $\bar{I}(\Lambda)$ was discussed in Ref. [5] and reference therein in the larger context of I-Love-Q relations. One of the hypothesis put forward to explain the EoS invariance of I-Love-Q relations was the lack of variability far from the core (low densities). The GP+astro set presents a unique crust while the meta model offers crust variability yet the former presents a slightly larger error on the fit of $\bar{I}(\Lambda)$ than the latter: we did not observe an obvious loss of invariance when including the nuclear physics constrained crust variability of the meta model.

Finally, from this hierarchy of universality between the different relations, we can anticipate that there exists a detector sensitivity for which the radius extraction from the measurement of the tidal deformability in a gravitational wave signal could be overcome by the EoS variability, while the extraction of the moment of inertia from the same signal would not.

B. Error marginalization

1. Radius from binary neutron star mergers

In Fig. 2, we present the extraction of the radius from the simulated gravitational wave signal of a binary neutron star merger using the relation $C(\Lambda)$; the O4 sensitivity is presented in orange and the Cosmic Explorer and Einstein telescope sensitivity is presented in green. Fig. 2a used the fit based on the meta-modeling set of EoS while Fig. 2b used the Gaussian process set.

The radius extraction using the Gaussian or the uniform marginalization of the error, or simply the fit line and without including any error, are (roughly) equivalent at O4 sensitivity. This fit limits (in shaded colors) are larger at that sensitivity but not significantly relative to the size of the contour, although it is more pronounced for the Gaussian process fit.

In the case of 3rd generation sensitivity, we first see that there is a significant difference between the Gaussian and uniform marginalization, as well as with the fit line without inclusion of the error: the Gaussian marginalization has overestimated the precision on the radius by around a factor of two compared to uniform marginalization. We can conclude that the technique used to include the error has an impact on the results in this sensitivity of the detectors. We also see on that figure that the extraction of the radius from the fit line is significantly thinner than the error marginalization: this indicates that the parameter extraction contours at that sensitivity are related to the fit error and not the tidal deformability recovery from the gravitational wave signal. This is confirmed by the limits of the error presented in shades of green: they are at the opposite ends of the uniform marginalization and do not overlap at all.

Finally, the meta-model (MM+ χ +PSR) fit offer a better precision on the parameter extraction than the Gaussian process (GP+astro) fit, as the maximum error presented in Table I indicated. This indicates that in parameter extraction, current astrophysical constraints are not equivalent to nuclear theory calculations in data-driven relations. We also note that higher radii are extracted for a given mass with the Gaussian process fit, in accordance with our discussion of Fig. 1a in Section III A.

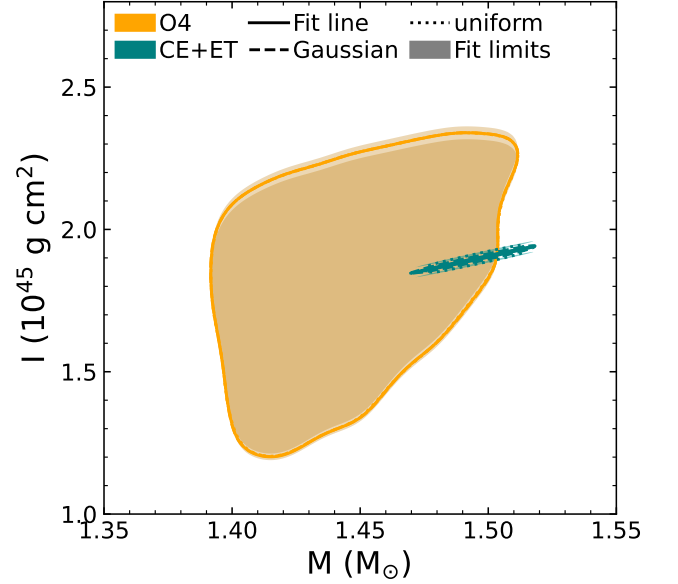


FIG. 3: $I(M)$ extracted from the $\bar{I}(\Lambda)$ relation and a simulated GW signal in the sensitivity of O4 (orange) and Cosmic Explorer and Einstein telescope (green); contours are shown at $1-\sigma$. Results are presented for the fit line (plain lines), with the Gaussian marginalization of the error (dashed line), and with the uniform marginalization of the error (dotted line); the limits of the error are presented in shades of colors. Fits used are that of GP+astro.

2. Moment of inertia from binary neutron star mergers

In Fig. 3, we present the extraction of the moment of inertia using the relation $\bar{I}(\Lambda)$ and the fit based on the Gaussian process set (which produces the largest fit error, see Table I). In that case, we can see that the two marginalization techniques, the limit of the error and the extraction from the fit line all overlap, both for O4 sensitivity and CE+ET sensitivity. This is not explained by the parameter estimation of the tidal deformability, as we use the same source and same set of EoS as for Fig. 2 but by the nature of the quasi-universality of the relation $\bar{I}(\Lambda)$. As can be seen in Fig. 1c, this relation presents a significant universality, which makes considerations of the marginalization technique, or even purely of the error, irrelevant. The error associated to the parameter estimation dominates whatever the sensitivity of the detector. We conclude that the universality of the relation $\bar{I}(\Lambda)$ will strongly hold with the 3rd generation of gravitational wave detectors.

3. Moment of inertia from X-ray detections

In Fig. 4, we present the extraction of the moment of inertia using the relation $\bar{I}(C)$. For the meta-model fits presented in Fig 4a, the marginalization technique does not impact the results. For the fits based on the

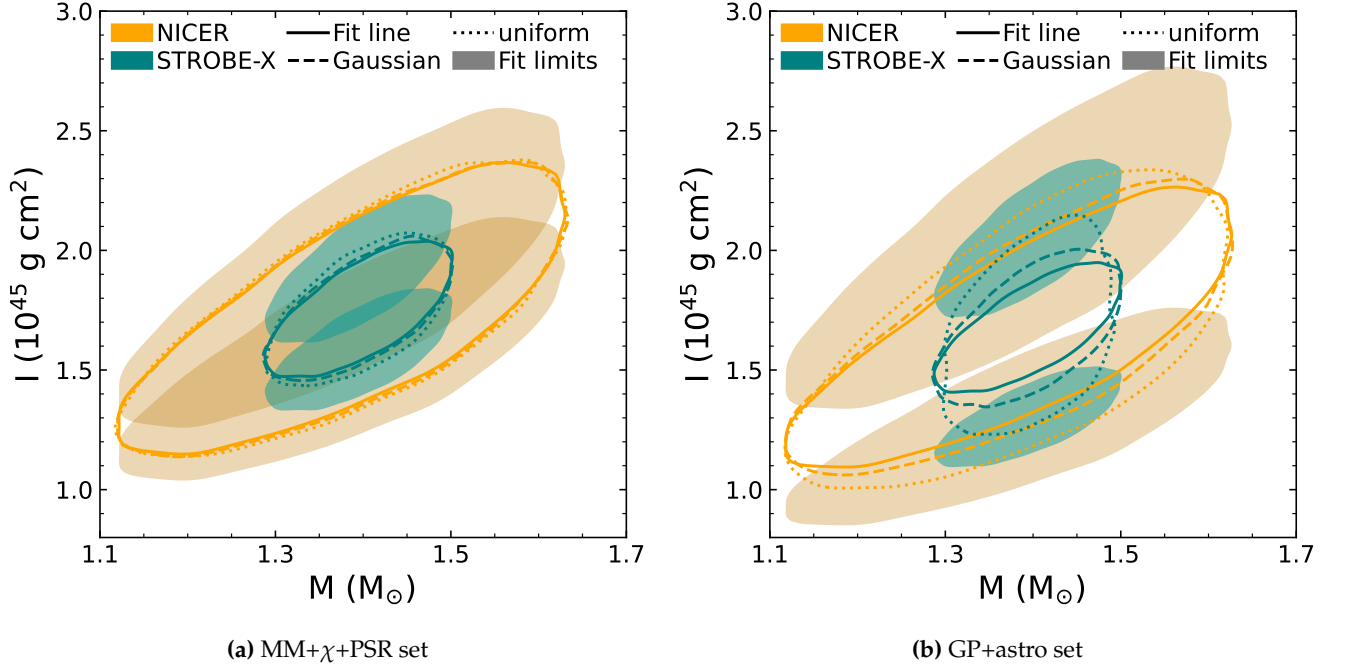


FIG. 4: $I(M)$ extracted from the $\bar{I}(C)$ relation and the simulated X-ray signal in the sensitivity of NICER (orange) and Strobe-X (green); contours are shown at $1\text{-}\sigma$. Results are presented for the fit line (plain lines), with the Gaussian marginalization of the error (dashed line), and with the uniform marginalization of the error (dotted line); the limits of the error are presented in shades of colors.

Gaussian process set presented in Fig. 4b, the results are impacted at high sensitivity (STROBE-X) as the Gaussian marginalization underestimates the error by almost a third compared to the uniform marginalization. The constraints brought forth by nuclear physics in the meta-modeling allow us to consider that STROBE-X sensitivity still dominates (or is at least equivalent) to the EoS variability of the meta-model based data-driven relation $\bar{I}(C)$.

C. Equation of state inference vs data-driven relations

1. Moment of inertia extraction

We show the moment of inertia distribution extracted with the EoS dependent relation $M(I)$ from the GP+astro and MM+ χ +PSR EoSs inferred on by the simulated STROBE-X source in Fig. 5a. We compare it to the moment of inertia distribution obtained with the data-driven relation fits which parameters are presented in Table I. The EoS inference leads to a better determination of the moment of inertia than the use of data-driven relation fits. In the case of the GP+astro set, the improvement is significant, while in the case of the meta-model it is almost equivalent: this is in accordance with results presented in Fig. 4. The peaks of the EoS inference distributions are not the same for the GP+astro and the meta-model set. The GP+astro

set is informed by GW170817 which softens the EoS distribution in that set while the meta-model set can explore stiffer models. The distribution for I determined by the data-driven relation of the GP+astro however explores higher values of the moment of inertia than its EoS inference counterpart. The fit established from a set of EoS informed by data (astrophysics or nuclear physics) does not keep memory distribution of that set: the fit only cares about the boundary points, not the distribution of points itself.

The moment of inertia distribution extracted with gravitational wave data simulated with Cosmic Explorer and Einstein Telescope sensitivity is presented in Fig. 5b. The extraction of I with the data-driven relation $\bar{I}(\Lambda)$ are very similar: as discussed in Fig. 1c, this relation is very universal, although we can better distinguish between the two different EoS sets. The difference of the peak's values in the EoS inference and data-driven relation distributions is also visible even though the distributions overlap well: the use of fits which loose prior information on the sets leads again to higher values of the moment of inertia, suggesting a slightly stiffer EoS. Finally, we also note that the 3G gravitational wave detection offer a better constraint on the moment of inertia than STROBE-X does with EoS inference.

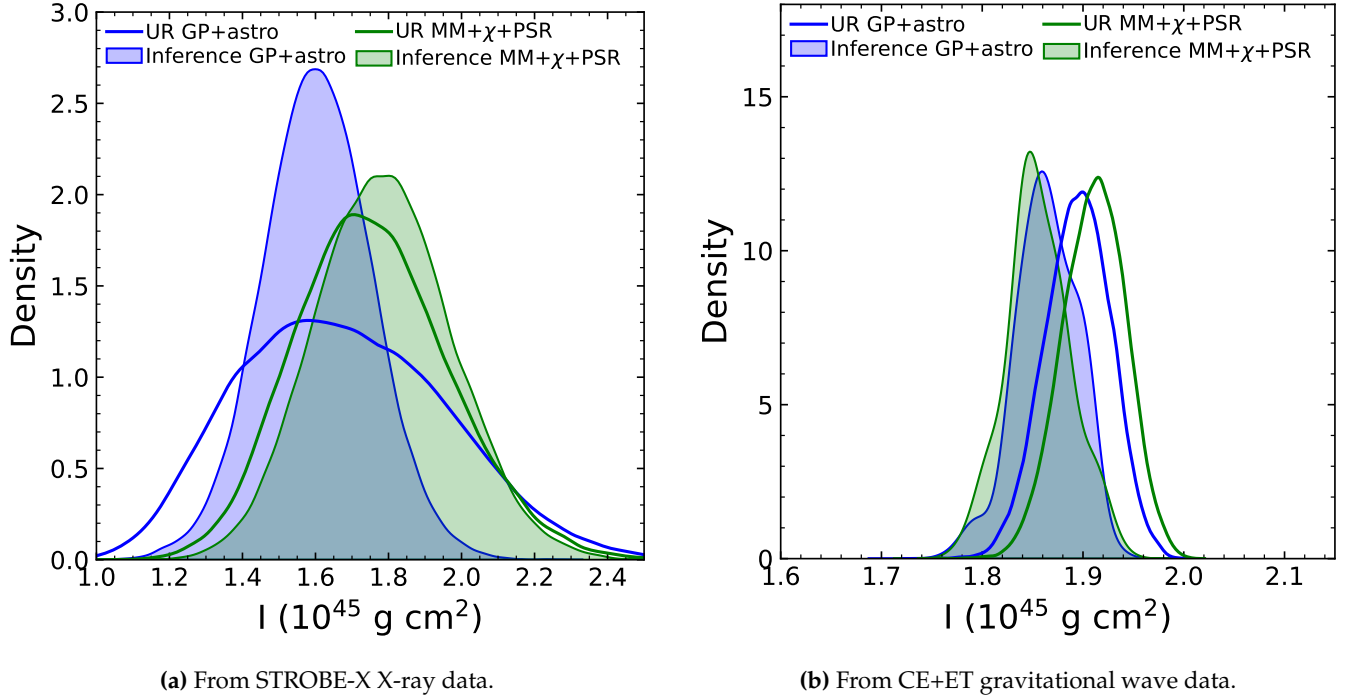


FIG. 5: Moment of inertia distribution from parameter extraction operated with data-driven relations and EoS inference.

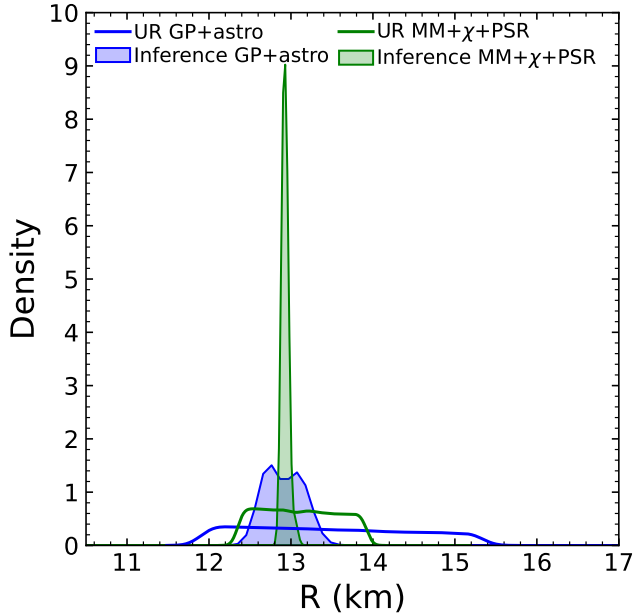


FIG. 6: Radius distribution from parameter extraction operated with data-driven relations and EoS inference.

2. Radius extraction

We show the radius distribution extracted with the EoS dependent relation $C(\Lambda)$ from the GP+astro and MM+ χ +PSR EoSs inferred on by the simulated

gravitational wave data source in Fig. 6. Results are similar to Fig. 5b, except that the distribution offered by data-driven relations is much larger. We also note that the meta model inference peak on the radius in Fig 6 is much more pronounced than the peak in moment of inertia of Fig. 5b. This is because the radius is strongly related to the description of the crust while the moment of inertia is mainly sensitive to the core. While the core treatment of the MM+ χ +PSR and the GP+astro seem to lead to similar distributions for the moment of inertia inference, this is not the case for the radius inference. The power of the low density treatment of the meta model explicitly shows in this case.

We also note that the distributions presented in Fig. 5 and Fig. 6 are not always very well resolved. In this paper, we have used pre-computed EoS sets. They will be an issue for future detectors and a generator of EoS set operating with the inference will be necessary to offer well resolved distributions.

IV. CONCLUSION

In this paper, we discuss three macroscopic parameter relations : $C(\Lambda)$, $\bar{I}(C)$ and $\bar{I}(\Lambda)$. We have studied the use of so called quasi-universal relations in moment of inertia and radius extraction from gravitational wave and X-ray signals with current and future detector sensitivity.

We have used three different sets of EoSs to design the relations and their associated fits. We have shown

that for compactness related relations discussed in this paper, the EoS variability lets us distinguish between the different sets of EoS while the $\bar{I}(\Lambda)$ presents a more pronounced universality. To accurately express the EoS set dependence of the relations, we refer to data-driven relation instead of quasi-universal relations.

We have discussed the fit error marginalization in parameter extraction and have shown that different approaches do not impact the result for O4 or NICER sensitivity, but do impact the result for Einstein Telescope and Cosmic Explorer and STROBE-X sensitivity.

Finally, we have shown that using data-driven relations in parameter extraction with the future detector sensitivity will lead to much larger uncertainties on the extracted parameter than direct EoS inference. In overall, when the quasi-universality of data-driven relations is overcome by the sensitivity of the detector and its consequent information on the EoS, using data-driven relations is sub-optimal.

In previous usage, data driven relations were broadly equivalent in parameter extraction when compared to direct EoS inference (for example, in GW170817 [21]). We show here that even if future data-driven relations are conditioned on EoS knowledge with precision measurement, direct usage of those EoSs will be more effective in extracting parameters.

ACKNOWLEDGMENTS

The authors thank Rory Smith, Sunny Ng, Philippe Landry, Carl-Johan Haster, Isaac Legred and Emily Wuchner for useful discussion about numerical applications. The authors thank collaborators of the Nuclear Physics from Multi-Messenger Mergers (NP3M) Focused Research Hub for useful discussions. The authors acknowledge the financial support of the National Science Foundation grant Number PHY 21-16686 and PHY 21-10441. The authors are grateful for computational resources provided by the LIGO Laboratory and supported by National Science Foundation Grants PHY-0757058 and PHY-0823459. Software: This work makes use of scipy [52], numpy [53] and matplotlib [54].

Appendix A: Mass, radius, moment of inertia and tidal deformability modeling

We study the astrophysical features of a non-rotating neutron star within the gravity theory of General Relativity, assuming the line element ds of a spherically symmetric, static and isotropic space-time determined by the metric $g_{\mu\nu}$ as

$$\begin{aligned} ds^2 &= g_{\mu\nu} dx^\mu dx^\nu \\ &= -e^{2\phi(r)} dt^2 + e^{2\lambda(r)} dr^2 + r^2 d\theta + r^2 \sin(\theta) d\phi^2, \end{aligned} \quad (A1)$$

with r the Schwarzschild like radial coordinate. Considering vacuum outside the neutron star, this metric reduces to the Schwarzschild one. Inside the star, the functions ϕ (gravitational redshift) and λ (radial gravitational distortion) are solved using hydrostatic equilibrium equations and the Equation of State (EoS) $P = P(\epsilon)$, with P the pressure and ϵ the energy density. In the assumption that the matter inside the neutron star is a perfect fluid, we obtain the Tolman-Oppenheimer-Volkov (TOV) differential equations

$$\frac{dm}{dr} = \frac{4\pi r^2}{c^2} \epsilon(r), \quad (A2)$$

$$\frac{d\phi}{dr} = \frac{Gm(r)}{r^2} \left(1 + \frac{4\pi r^3 P(r)}{m(r)c^2} \right) \left(1 - \frac{2Gm(r)}{rc^2} \right)^{-1}, \quad (A3)$$

$$\frac{dP}{dr} = - \left(\frac{\epsilon(r) + P(r)}{c^2} \right) \frac{d\phi}{dr}, \quad (A4)$$

with G the gravitational constant, c the speed of light and $m(r)$ the gravitational mass radial profile. The central energy density or central pressure, used as a boundary condition to solve the TOV equations, determines the total gravitational mass M and the total radius R of the neutron star.

The dimensionless tidal deformability expresses the quadrupole moment response induced on the neutron star by an external gravitational field. Its value at the surface of the star denoted $\Lambda = \lambda_2(R)$ is given by the tidal deformability radial profile

$$\lambda_2(r) = \frac{2}{3} k_2(r) C(r)^{-5}, \quad (A5)$$

with $C(r) = Gm(r)/(rc^2)$ the compactness of a star of radius r . The tidal Love number k_2 is given by

$$\begin{aligned} k_2(r) &= \frac{8C(r)^5}{5} (1 - 2C(r))^2 [2 + 2C(r)(y(r) - 1) - y(r)] \\ &\quad \times \left(2C(r) [6 - 3y(r) + 3C(r)(5y(r) - 8)] \right. \\ &\quad \left. + 4C(r)^3 [13 - 11y(r) + C(r)(3y(r) - 2) \right. \\ &\quad \left. + 2C(r)^2 (1 + y(r))] \right. \\ &\quad \left. + 3(1 - 2C(r))^2 [2 - y(r) + 2C(r)(y(r) - 1)] \right. \\ &\quad \left. \ln(1 - 2C(r)) \right)^{-1}, \end{aligned} \quad (A6)$$

see, e.g., Ref. [20] and reference therein. The function $y(r)$ is to be solved simultaneously with the TOV equations using the additional differential equation [20, 55]

$$r \frac{dy}{dr} + y(r)^2 + F(r)y(r) + Q(r) = 0, \quad (A7)$$

with the boundary condition $y(0) = 2$, see Section IV.A of Ref. [56]. The functions $F(r)$ and $Q(r)$ are given by

$$F(r) = \left(1 - \frac{4\pi G}{c^2} r^2 \frac{\epsilon(r) - P(r)}{c^2}\right) \left(1 - \frac{2Gm(r)}{rc^2}\right)^{-1}, \quad (\text{A8})$$

$$Q(r) = \frac{4\pi G}{c^2} r^2 \left(1 - \frac{2Gm(r)}{rc^2}\right)^{-1} \left[\frac{5\epsilon(r) + 9P(r)}{c^2} + \frac{\epsilon(r) + P(r)}{c_s(r)^2} - \frac{6c^2}{4\pi G r^2} \right] - 4 \left(\frac{Gm(r)}{rc^2} + \frac{4\pi G}{c^4} r^2 P(r) \right)^2 \left(1 - \frac{2Gm(r)}{rc^2}\right)^{-2} \quad (\text{A9})$$

with c_s the sound speed that should be treated with caution around a discontinuous density, see, e.g., Ref. [57].

To model the moment of inertia, we use the slow and rigid rotation approximation detailed in Ref. [19]⁶. When considering rigid rotation, the uniform angular frequency is contributed to by the local spin frequency $\omega(r)$ and the angular momentum $j(r)$ of a sphere of radius r . We denote Ω the uniform angular frequency of the star, defined at the surface ($r = R$) as

$$\Omega = \omega(R) + \frac{2Gj(R)}{c^2 R^3}. \quad (\text{A10})$$

The uniform angular frequency, the angular momentum

and the moment of inertia are solution of the differential equations

$$\frac{dI}{dr} = \frac{8\pi}{3} \frac{r^4}{e^{\Phi(r)}} \frac{\omega(r) \epsilon(r) + P(r)}{c^2} \left(1 - \frac{2Gm(r)}{c^2 r}\right)^{-1/2}, \quad (\text{A11})$$

$$\frac{d\omega(r)}{dr} = \frac{6G}{c^2} \frac{e^{\Phi(r)}}{r^4} j(r) \left(1 - \frac{2Gm(r)}{c^2 r}\right)^{-1/2}, \quad (\text{A12})$$

$$\frac{dj(r)}{dr} = \frac{8\pi}{3} \frac{r^4}{e^{\Phi(r)}} \omega(r) \frac{\epsilon(r) + P(r)}{c^2} \left(1 - \frac{2Gm(r)}{c^2 r}\right)^{-1/2}, \quad (\text{A13})$$

to be solved simultaneously with the TOV equations.

Appendix B: Distribution of EoSs in the sets

We present in Fig. 7 the distribution of compactness and dimensionless moment of inertia points for GP+atmo and MM+ χ +PSR set.

Appendix C: Fit parameters and errors associated to the fits

We present in Table I the parameters of the fit for the relations presented in Section II C 2 and the maximum error associated to the fits with the different EoS sets presented in this paper.

-
- [1] K. Yagi and N. Yunes, Phys. Rev. D **88**, 023009 (2013), arXiv:1303.1528 [gr-qc].
 - [2] B. Haskell, R. Ciolfi, F. Pannarale, and L. Rezzolla, Monthly Notices of Royal Astronomical Society **438**, L71 (2014), arXiv:1309.3885 [astro-ph.SR].
 - [3] S. Chakrabarti, T. Delsate, N. G rlebeck, and J. Steinhoff, Physical Review Letters **112**, 201102 (2014), arXiv:1311.6509 [gr-qc].
 - [4] D. D. Doneva, S. S. Yazadjiev, and K. D. Kokkotas, Physical Review D **92**, 064015 (2015), arXiv:1507.00378 [gr-qc].
 - [5] K. Yagi and N. Yunes, Physics Reports **681**, 1 (2017), arXiv:1608.02582 [gr-qc].
 - [6] M. C. Miller, F. K. Lamb, A. J. Dittmann, S. Bogdanov, Z. Arzoumanian, K. C. Gendreau, S. Guillot, A. K. Harding, W. C. G. Ho, J. M. Lattimer, R. M. Ludlam, S. Mahmoodifar, S. M. Morsink, P. S. Ray, T. E. Strohmayer, K. S. Wood, T. Enoto, R. Foster, T. Okajima,

- G. Prigozhin, and Y. Soong, Astrophysical Journal, Letters **887**, L24 (2019), arXiv:1912.05705 [astro-ph.HE].
- [7] T. E. Riley, A. L. Watts, S. Bogdanov, P. S. Ray, R. M. Ludlam, S. Guillot, Z. Arzoumanian, C. L. Baker, A. V. Bilous, D. Chakrabarty, K. C. Gendreau, A. K. Harding, W. C. G. Ho, J. M. Lattimer, S. M. Morsink, and T. E. Strohmayer, The Astrophysical Journal **887**, L21 (2019).
- [8] M. C. Miller, F. K. Lamb, A. J. Dittmann, S. Bogdanov, Z. Arzoumanian, K. C. Gendreau, S. Guillot, W. C. G. Ho, J. M. Lattimer, M. Loewenstein, S. M. Morsink, P. S. Ray, M. T. Wolff, C. L. Baker, T. Cazeau, S. Manthripragada, C. B. Markwardt, T. Okajima, S. Pollard, I. Cognard, H. T. Cromartie, E. Fonseca, L. Guillemot, M. Kerr, A. Parthasarathy, T. T. Pennucci, S. Ransom, and I. Stairs, Astrophysical Journal, Letters **918**, L28 (2021), arXiv:2105.06979 [astro-ph.HE].
- [9] T. E. Riley, A. L. Watts, P. S. Ray, S. Bogdanov, S. Guillot, S. M. Morsink, A. V. Bilous, Z. Arzoumanian, D. Choudhury, J. S. Deneva, K. C. Gendreau, A. K. Harding, W. C. G. Ho, J. M. Lattimer, M. Loewenstein, R. M. Ludlam, C. B. Markwardt, T. Okajima, C. Prescod-Weinstein, R. A. Remillard, M. T. Wolff, E. Fonseca, H. T. Cromartie, M. Kerr, T. T. Pennucci, A. Parthasarathy, S. Ransom, I. Stairs, L. Guillemot, and I. Cognard, Astrophysical Journal, Letters **918**, L27 (2021), arXiv:2105.06980 [astro-ph.HE].

⁶ Modeling the moment of inertia outside of this approximation requires solving the Einstein's equations with a metric describing a stationary and axisymmetric space-time, see, e.g., the LORENE library.

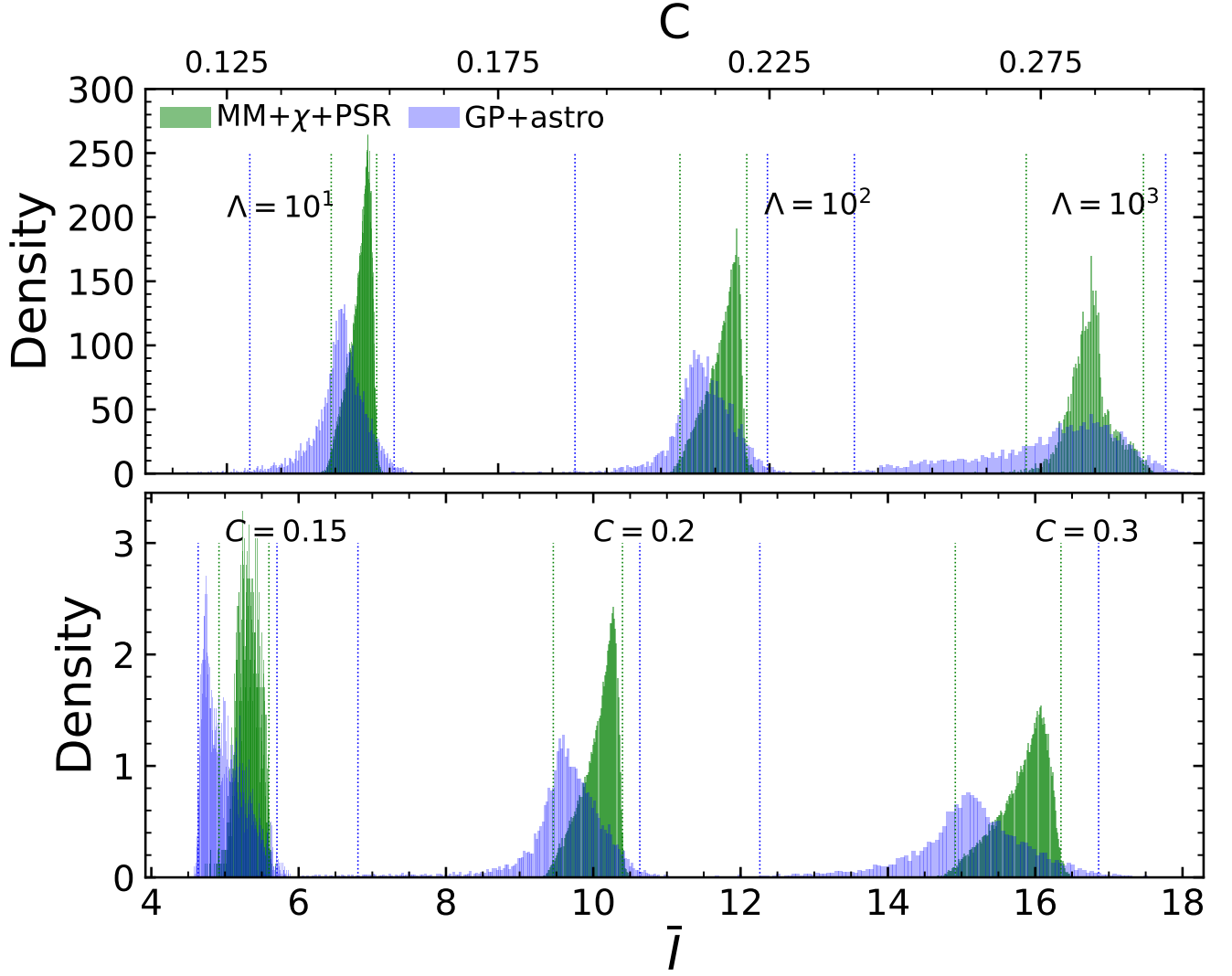


FIG. 7: Distribution of points of compactness (top) and dimensionless moment of inertia (bottom) for a few values of the tidal deformability and compactness respectively, in MM+ χ +PSR and GP+astro sets. Vertical lines correspond to the 99 percentile limits of the distributions.

Relation	Set	a_0	a_1	a_2	a_3	a_4	a_5	Δ_{\max} (in %)
$C(\Lambda)$	GP+astro	3.7678×10^{-1}	-5.1851×10^{-2}	8.3659×10^{-3}	-1.6529×10^{-3}	1.5470×10^{-4}	-5.0440×10^{-6}	12.6129
	Nuclear	3.5636×10^{-1}	-3.6950×10^{-2}	4.5372×10^{-3}	-1.1316×10^{-3}	1.1773×10^{-4}	-4.0028×10^{-6}	5.9967
	MM+ χ +PSR	3.3888×10^{-1}	-1.0262×10^{-2}	-9.8856×10^{-3}	2.0656×10^{-3}	-1.9511×10^{-4}	7.2814×10^{-6}	5.2443
$\bar{I}(\Lambda)$	GP+astro	1.5011×10^0	5.2134×10^{-2}	2.4508×10^{-2}	-9.9877×10^{-4}	2.7064×10^{-5}	-3.3703×10^{-7}	0.9699
	Nuclear	1.4874×10^0	6.9698×10^{-2}	1.9206×10^{-2}	-2.5145×10^{-4}	-2.0918×10^{-5}	7.4502×10^{-7}	0.6774
	MM+ χ +PSR	1.4857×10^0	6.7440×10^{-2}	1.8129×10^{-2}	2.2972×10^{-4}	-7.7256×10^{-5}	2.8044×10^{-6}	0.5033
$\bar{I}(C)$	GP+astro	1.5333×10^1	-1.1303×10^1	3.8536×10^0	-5.0621×10^{-1}	3.2323×10^{-2}	-7.5871×10^{-4}	22.2608
	Nuclear	6.1602×10^0	-4.7746×10^0	2.1004×10^0	-2.8280×10^{-1}	1.9466×10^{-2}	-4.9244×10^{-4}	9.6337
	MM+ χ +PSR	2.3584×10^0	1.9423×10^{-1}	-4.5225×10^{-2}	1.1677×10^{-1}	-1.4423×10^{-2}	5.7714×10^{-4}	9.1280

TABLE I: Fit parameters of the relation $C(\Lambda)$, $\bar{I}(C)$ and $\bar{I}(\Lambda)$ based on the parametrization presented in Eqs. (1), (2), (3), and maximum error associated to the fit Δ_{\max} . Results are presented for the EoS sets discussed in this paper, GP+astro, the nuclear set and the MM+ χ +PSR.

- [10] P. Ray and et al., in *Bulletin of the American Astronomical Society*, arXiv:1304.2052 [gr-qc]. Vol. 51 (2019) p. 231.
- [11] B. P. Abbott, LIGO Scientific Collaboration, and Virgo Collaboration, *Physical Review Letters* **119**, 161101 (2017), arXiv:1710.05832 [gr-qc].
- [12] M. Evans, R. X. Adhikari, C. Afle, S. W. Ballmer, S. Biscoveanu, S. Borhanian, D. A. Brown, Y. Chen, R. Eisenstein, A. Gruson, A. Gupta, and others, arXiv e-prints, arXiv:2109.09882 (2021), arXiv:2109.09882 [astro-ph.IM].
- [13] M. Maggiore, C. V. D. Broeck, N. Bartolo, E. Belgacem, D. Bertacca, M. A. Bizouard, M. Branchesi, S. Clesse, S. Foffa, J. García-Bellido, and others, *Journal of Cosmology and Astroparticle Physics* **2020**, 050–050 (2020).
- [14] M. Branchesi, M. Maggiore, D. Alonso, C. Badger, B. Banerjee, F. Beirnaert, E. Belgacem, S. Bhagwat, G. Boileau, S. Borhanian, D. D. Brown, M. Leong Chan, G. Cusin, S. L. Danilishin, J. Degallaix, V. De Luca, A. Dhani, T. Dietrich, U. Dupletsa, S. Foffa, G. Franciolini, A. Freise, G. Gemme, B. Goncharov, A. Ghosh, F. Gulminelli, I. Gupta, P. Kumar Gupta, J. Harms, N. Hazra, S. Hild, T. Hinderer, I. Siong Heng, F. Iacovelli, J. Janquart, K. Janssens, A. C. Jenkins, C. Kalaghatgi, X. Korovesi, T. G. F. Li, Y. Li, E. Loffredo, E. Maggio, M. Mancarella, M. Mapelli, K. Martinovic, A. Maselli, P. Meyers, A. L. Miller, C. Mondal, N. Muttoni, H. Narola, M. Oertel, G. Oganessian, C. Pacilio, C. Palomba, P. Pani, A. Pasqualetti, A. Perego, C. Pérois, M. Pieroni, O. J. Piccinni, A. Puecher, P. Puppo, A. Ricciardone, A. Riotto, S. Ronchini, M. Sakellariadou, A. Samajdar, F. Santoliquido, B. S. Sathyaprakash, J. Steinlechner, S. Steinlechner, A. Utina, C. Van Den Broeck, and T. Zhang, *Journal of Cosmology and Astroparticle Physics* **2023**, 068 (2023), arXiv:2303.15923 [gr-qc].
- [15] M. Kramer, I. H. Stairs, R. N. Manchester, N. Wex, A. T. Deller, W. A. Coles, M. Ali, M. Burgay, F. Camilo, I. Cognard, T. Damour, G. Desvignes, R. D. Ferdman, P. C. C. Freire, S. Grondin, L. Guillemot, G. B. Hobbs, G. Janssen, R. Karuppusamy, D. R. Lorimer, A. G. Lyne, J. W. McKee, M. McLaughlin, L. E. Münch, B. B. P. Perera, N. Pol, A. Possenti, J. Sarkissian, B. W. Stappers, and G. Theureau, *Physical Review X* **11**, 041050 (2021), arXiv:2112.06795 [astro-ph.HE].
- [16] P. Landry and B. Kumar, *The Astrophysical Journal Letters* **868**, L22 (2018), arXiv:1807.04727 [gr-qc].
- [17] R. C. Tolman, *Physical Review* **55**, 364 (1939).
- [18] J. R. Oppenheimer and G. M. Volkoff, *Physical Review* **55**, 374 (1939).
- [19] J. B. Hartle, *The Astrophysical Journal* **150**, 1005 (1967).
- [20] T. Hinderer, *Astrophysical Journal* **677**, 1216 (2008), arXiv:0711.2420 [astro-ph].
- [21] B. P. Abbott, LIGO Scientific Collaboration, and Virgo Collaboration, *Physical Review Letters* **121**, 161101 (2018), arXiv:1805.11581 [gr-qc].
- [22] H. O. Silva, A. M. Holgado, A. Cárdenas-Avendaño, and N. Yunes, *Physical Review Letters* **126**, 181101 (2021), arXiv:2004.01253 [gr-qc].
- [23] I. Legred, B. O. Sy-Garcia, K. Chatziioannou, and R. Essick, “Assessing equation of state-independent relations for neutron stars with nonparametric models,” (2023), arXiv:2310.10854 [astro-ph.HE].
- [24] A. Maselli, V. Cardoso, V. Ferrari, L. Gualtieri, and P. Pani, *Physical Review D* **88**, 023007 (2013),
- [25] D. A. Godzieba, R. Gamba, D. Radice, and S. Bernuzzi, *Physical Review D* **103**, 063036 (2021), arXiv:2012.12151 [astro-ph.HE].
- [26] C. Breu and L. Rezzolla, *Mon. Not. Roy. Astron. Soc.* **459**, 646 (2016), arXiv:1601.06083 [gr-qc].
- [27] K. Yagi and N. Yunes, *Classical and Quantum Gravity* **33**, 13LT01 (2016), arXiv:1512.02639 [gr-qc].
- [28] L. Suleiman, M. Fortin, J. L. Zdunik, and C. Providência, *Physical Review C* **106**, 035805 (2022), arXiv:2209.06052 [nucl-th].
- [29] R. C. Pereira, P. Costa, and C. Providência, *Physical Review D* **94**, 094001 (2016), arXiv:1610.06435 [nucl-th].
- [30] A. Sedrakian, J. J. Li, and F. Weber, *Progress in Particle and Nuclear Physics* **131**, 104041 (2023), arXiv:2212.01086 [nucl-th].
- [31] G. Baym, T. Hatsuda, T. Kojo, P. D. Powell, Y. Song, and T. Takatsuka, *Reports on Progress in Physics* **81**, 056902 (2018), arXiv:1707.04966 [astro-ph.HE].
- [32] E. Annala, T. Gorda, A. Kurkela, J. Nättilä, and A. Vuorinen, *Nature Physics* **16**, 907 (2020), arXiv:1903.09121 [astro-ph.HE].
- [33] L. Suleiman, M. Fortin, J. L. Zdunik, and P. Haensel, *Physical Review C* **104**, 015801 (2021), arXiv:2106.12845 [astro-ph.HE].
- [34] M. V. Beznogov and D. G. Yakovlev, *Monthly Notices of Royal Astronomical Society* **452**, 540 (2015), arXiv:1507.04206 [astro-ph.SR].
- [35] E. Fonseca, H. T. Cromartie, T. T. Pennucci, P. S. Ray, A. Y. Kirichenko, S. M. Ransom, P. B. Demorest, I. H. Stairs, Z. Arzoumanian, L. Guillemot, A. Parthasarathy, M. Kerr, I. Cognard, P. T. Baker, H. Blumer, P. R. Brook, M. DeCesar, T. Dolch, F. A. Dong, E. C. Ferrara, W. Fiore, N. Garver-Daniels, D. C. Good, R. Jennings, M. L. Jones, V. M. Kaspi, M. T. Lam, D. R. Lorimer, J. Luo, A. McEwen, J. W. McKee, M. A. McLaughlin, N. Mann, B. W. Meyers, A. Naidu, C. Ng, D. J. Nice, N. Pol, H. A. Radovan, B. Shapiro-Albert, C. M. Tan, S. P. Tendulkar, J. K. Swiggum, H. M. Wahl, and W. W. Zhu, *The Astrophysical Journal Letters* **915**, L12 (2021), arXiv:2104.00880 [astro-ph.HE].
- [36] Z. Arzoumanian, A. Brazier, S. Burke-Spolaor, S. Chamberlin, S. Chatterjee, B. Christy, J. M. Cordes, N. J. Cornish, F. Crawford, H. T. Cromartie, K. Crowter, M. E. DeCesar, P. B. Demorest, T. Dolch, J. A. Ellis, R. D. Ferdman, E. C. Ferrara, E. Fonseca, N. Garver-Daniels, P. A. Gentile, D. Halmrast, E. A. Huerta, F. A. Jenet, C. Jessup, G. Jones, M. L. Jones, D. L. Kaplan, M. T. Lam, T. J. W. Lazio, L. Levin, A. Lommen, D. R. Lorimer, J. Luo, R. S. Lynch, D. Madison, A. M. Matthews, M. A. McLaughlin, S. T. McWilliams, C. Mingarelli, C. Ng, D. J. Nice, T. T. Pennucci, S. M. Ransom, P. S. Ray, X. Siemens, J. Simon, R. Spiewak, I. H. Stairs, D. R. Stinebring, K. Stovall, J. K. Swiggum, S. R. Taylor, M. Vallisneri, R. van Haasteren, S. J. Vigeland, and W. Z. and, *The Astrophysical Journal Supplement Series* **235**, 37 (2018).
- [37] P. J. Davis, H. Dinh Thi, A. F. Fantina, F. Gulminelli, M. Oertel, and L. Suleiman, “Inference of neutron-star properties with unified crust-core equations of state for parameter estimation,” (2023), submitted.
- [38] C. Drischler, K. Hebeler, and A. Schwenk, *Physical Review C* **93**, 054314 (2016), arXiv:1510.06728 [nucl-th].
- [39] J. Margueron, R. Hoffmann Casali, and F. Gulminelli, *Physical Review C* **97**, 025805 (2018), arXiv:1708.06894

- [nucl-th].
- [40] R. Essick, P. Landry, and D. E. Holz, *Physical Review D* **101**, 063007 (2020), arXiv:1910.09740 [astro-ph.HE].
 - [41] F. Douchin and P. Haensel, *Astron. Astrophys.* **380**, 151 (2001), arXiv:astro-ph/0111092 [astro-ph].
 - [42] G. Ashton, M. Hübner, P. D. Lasky, C. Talbot, K. Ackley, S. Biscoveanu, Q. Chu, A. Divakarla, P. J. Easter, B. Goncharov, F. Hernandez Vivanco, J. Harms, M. E. Lower, G. D. Meadors, D. Melchor, E. Payne, M. D. Pitkin, J. Powell, N. Sarin, R. J. E. Smith, and E. Thrane, *The Astrophysical Journal Supplement Series* **241**, 27 (2019), arXiv:1811.02042 [astro-ph.IM].
 - [43] R. Smith, S. E. Field, K. Blackburn, C.-J. Haster, M. Pürrer, V. Raymond, and P. Schmidt, *Physical Review D* **94**, 044031 (2016), arXiv:1604.08253 [gr-qc].
 - [44] R. Smith, S. Borhanian, B. Sathyaprakash, F. Hernandez Vivanco, S. E. Field, P. Lasky, I. Mandel, S. Morisaki, D. Ottaway, B. J. J. Slagmolen, E. Thrane, D. Töyrä, and S. Vitale, *Physical Review Letters* **127**, 081102 (2021), arXiv:2103.12274 [gr-qc].
 - [45] S. Typel, G. Röpke, T. Klähn, D. Blaschke, and H. H. Wolter, *Physical Review C* **81**, 015803 (2010), arXiv:0908.2344 [nucl-th].
 - [46] S. Hild, M. Abernathy, F. Acernese, P. Amaro-Seoane, N. Andersson, K. Arun, F. Barone, B. Barr, M. Barsuglia, M. Beker, N. Beveridge, S. Birindelli, S. Bose, L. Bosi, S. Braccini, C. Bradaschia, T. Bulik, E. Calloni, G. Cella, E. Chassande Mottin, S. Chelkowski, A. Chincarini, J. Clark, E. Coccia, C. Colacino, J. Colas, A. Cumming, L. Cunningham, E. Cuoco, S. Danilishin, K. Danzmann, R. De Salvo, T. Dent, R. De Rosa, L. Di Fiore, A. Di Virgilio, M. Doets, V. Fafone, P. Falferi, R. Flaminio, J. Franc, F. Frasconi, A. Freise, D. Friedrich, P. Fulda, J. Gair, G. Gemme, E. Genin, A. Gennai, A. Giazotto, K. Glampedakis, C. Gräf, M. Granata, H. Grote, G. Guidi, A. Gurkovsky, G. Hammond, M. Hannam, J. Harms, D. Heinert, M. Hendry, I. Heng, E. Hennes, J. Hough, S. Husa, S. Huttner, G. Jones, F. Khalili, K. Kokeyama, K. Kokkotas, B. Krishnan, T. G. F. Li, M. Lorenzini, H. Lück, E. Majorana, I. Mandel, V. Mandic, M. Mantovani, I. Martin, C. Michel, Y. Minenkov, N. Morgado, S. Mosca, B. Mours, H. Müller-Ebhardt, P. Murray, R. Nawrodt, J. Nelson, R. Oshaughnessy, C. D. Ott, C. Palomba, A. Paoli, G. Parguez, A. Pasqualetti, R. Passaquieti, D. Passuello, L. Pinard, W. Plastino, R. Poggiani, P. Popolizio, M. Prato, M. Punturo, P. Puppo, D. Rabeling, P. Rapagnani, J. Read, T. Regimbau, H. Rehbein, S. Reid, F. Ricci, F. Richard, A. Rocchi, S. Rowan, A. Rüdiger, L. Santamaría, B. Sassolas, B. Sathyaprakash, R. Schnabel, C. Schwarz, P. Seidel, A. Sintes, K. Somiya, F. Speirits, K. Strain, S. Strigin, P. Sutton, S. Tarabrin, A. Thüring, J. van den Brand, M. van Veggel, C. van den Broeck, A. Vecchio, J. Veitch, F. Vetranò, A. Vicere, S. Vyatchanin, B. Willke, G. Woan, and K. Yamamoto, *Classical and Quantum Gravity* **28**, 094013 (2011), arXiv:1012.0908 [gr-qc].
 - [47] K. Chatziioannou, C.-J. Haster, and A. Zimmerman, *Phys. Rev. D* **97**, 104036 (2018), arXiv:1804.03221 [gr-qc].
 - [48] P. Landry and R. Essick, *Physical Review D* **99**, 084049 (2019), arXiv:1811.12529 [gr-qc].
 - [49] P. Landry, R. Essick, and K. Chatziioannou, *Physical Review D* **101**, 123007 (2020), arXiv:2003.04880 [astro-ph.HE].
 - [50] I. Legred, K. Chatziioannou, R. Essick, S. Han, and P. Landry, *Physical Review D* **104**, 063003 (2021), arXiv:2106.05313 [astro-ph.HE].
 - [51] R. B. Wiringa, V. Fiks, and A. Fabrocini, *Physical Review C* **38**, 1010 (1988).
 - [52] P. Virtanen, R. Gommers, T. E. Oliphant, M. Haberland, T. Reddy, D. Cournapeau, E. Burovski, P. Peterson, W. Weckesser, J. Bright, S. J. van der Walt, M. Brett, J. Wilson, K. J. Millman, N. Mayorov, A. R. J. Nelson, E. Jones, R. Kern, E. Larson, C. J. Carey, Í. Polat, Y. Feng, E. W. Moore, J. VanderPlas, D. Laxalde, J. Perktold, R. Cimrman, I. Henriksen, E. A. Quintero, C. R. Harris, A. M. Archibald, A. H. Ribeiro, F. Pedregosa, P. van Mulbregt, and SciPy 1.0 Contributors, *Nature Methods* **17**, 261 (2020), arXiv:1907.10121 [cs.MS].
 - [53] C. R. Harris, K. J. Millman, S. J. van der Walt, R. Gommers, P. Virtanen, D. Cournapeau, E. Wieser, J. Taylor, S. Berg, N. J. Smith, R. Kern, M. Picus, S. Hoyer, M. H. van Kerkwijk, M. Brett, A. Haldane, J. F. del Río, M. Wiebe, P. Peterson, P. Gérard-Marchant, K. Sheppard, T. Reddy, W. Weckesser, H. Abbasi, C. Gohlke, and T. E. Oliphant, *Nature* **585**, 357 (2020).
 - [54] J. D. Hunter, *Computing in Science and Engineering* **9**, 90 (2007).
 - [55] S. Postnikov, M. Prakash, and J. M. Lattimer, *Physical Review D* **82**, 024016 (2010), arXiv:1004.5098 [astro-ph.SR].
 - [56] T. Damour and A. Nagar, *Physical Review D* **80**, 084035 (2009), arXiv:0906.0096 [gr-qc].
 - [57] J. Takátsy and P. Kovács, *Physical Review D* **102**, 028501 (2020), arXiv:2007.01139 [astro-ph.HE].